

# Silver Makes Better Electrical Contacts to Thiol-Terminated Silanes than Gold

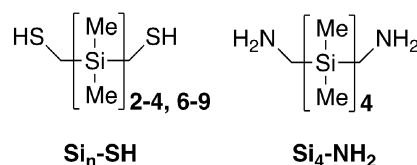
Haixing Li<sup>†</sup>, Timothy A. Su<sup>†</sup>, María Camarasa-Gómez<sup>†</sup>, Daniel Hernangómez-Pérez, Simon E. Henn, Vladislav Pokorný, Caravaggio D. Caniglia, Michael S. Inkpen, Richard Korytár, Michael L. Steigerwald,\* Colin Nuckolls,\* Ferdinand Evers,\* and Latha Venkataraman\*

**Abstract:** We report that the single-molecule junction conductance of thiol-terminated silanes with Ag electrodes are higher than the conductance of those formed with Au electrodes. These results are in contrast to the trends in the metal work function  $\Phi(\text{Ag}) < \Phi(\text{Au})$ . As such, a better alignment of the Au Fermi level to the molecular orbital of silane that mediates charge transport would be expected. This conductance trend is reversed when we replace the thiols with amines, highlighting the impact of metal–S covalent and metal–NH<sub>2</sub> dative bonds in controlling the molecular conductance. Density functional theory calculations elucidate the crucial role of the chemical linkers in determining the level alignment when molecules are attached to different metal contacts. We also demonstrate that conductance of thiol-terminated silanes with Pt electrodes is lower than the ones formed with Au and Ag electrodes, again in contrast to the trends in the metal work-functions.

The fundamental conductance properties of single molecules are most often probed with gold electrodes, as Au is both malleable and chemically inert under ambient conditions. The use of other metals as the electrical contacts in molecular electronics can offer new platforms for investigating the properties of molecular junctions. For instance, Ag and Pt can

potentially enable in situ chemical reactions that can influence the bridging organic molecules.<sup>[1]</sup> The density of states and optical properties of Ag and Pt, differing from Au, can open up new approaches in understanding electron transport through molecular junctions under illumination.<sup>[2]</sup> Relativistic effects in metal atoms, important in heavy elements, can also affect the metal–molecule interaction and influence the charge transport.<sup>[3]</sup> Although recent studies have shown that Ag,<sup>[4]</sup> Pt,<sup>[5]</sup> Cu,<sup>[4c,d]</sup> and Pd<sup>[5c,6]</sup> can be used as contacts to form single-molecule junctions, only a limited set of molecules have been shown to form stable junctions with these metals when compared with Au, especially under ambient conditions.

Herein, we describe conductance properties of a series of methylthiol- (Si<sub>n</sub>-SH) and methylamino- (Si<sub>4</sub>-NH<sub>2</sub>) termi-



nated permethyloligosilanes attached to Ag, Au, and Pt electrodes using the scanning tunneling microscope-based break junction (STM-BJ) technique.<sup>[7]</sup> Thiols are known to form covalent links with Au electrodes,<sup>[8]</sup> and can also bind to Ag and Pt electrodes by forming Ag–S and Pt–S covalent bonds. The important result we report here is that thiol-terminated silanes and alkanes display a higher conductance when bound to Ag than Au. Through density functional theory (DFT) calculations, we find that the alignment of metal Fermi level to highest occupied molecular orbital (HOMO) is similar for Ag–S and Au–S linked junctions. We find, however, that the orbital with most weight on the metal–S bond (the metal–S gateway state) is closer to the metal Fermi level in the case of Ag when compared with Au. The higher-lying gateway state and a close alignment of HOMO orbital with the metal Fermi level for Ag contribute to the higher conductance value we observe. By contrast, experiments and calculations on Ag–NH<sub>2</sub> and Au–NH<sub>2</sub> linked silane and alkane<sup>[4b]</sup> junctions show the reverse trend where Ag–NH<sub>2</sub> linked junctions having a lower conductance than Au–NH<sub>2</sub> linked ones. It is important to note that the charge-transport measurements on alkane–dithiol,<sup>[9]</sup> oligophenylene–dithiol,<sup>[10]</sup> and oligoacene–dithiol<sup>[11]</sup> monolayers formed

[\*] H. Li,<sup>[†]</sup> T. A. Su,<sup>[†]</sup> S. E. Henn, C. D. Caniglia, M. S. Inkpen, Dr. M. L. Steigerwald, Prof. C. Nuckolls, Prof. L. Venkataraman  
Department of Applied Physics and Chemistry  
Columbia University  
New York, NY 10027 (USA)  
E-mail: mls2064@columbia.edu  
cn37@columbia.edu  
lv2117@columbia.edu

M. Camarasa-Gómez,<sup>[†]</sup> Dr. D. Hernangómez-Pérez, Prof. F. Evers  
Institute of Theoretical Physics  
University of Regensburg  
93040 Regensburg (Germany)  
E-mail: ferdinand.evers@physik.uni-regensburg.de

Dr. V. Pokorný, Prof. R. Korytár  
Department of Condensed Matter Physics, Faculty of Math and Physics, Charles University  
Ke Karlovu 5, 121 16 Praha 2 (Czech Republic)

Dr. V. Pokorný  
Institute of Physics, The Czech Academy of Sciences  
Na Slovance 2, 18221 Prague 8 (Czech Republic)

[†] These authors contributed equally to this work.

Supporting information and the ORCID identification number(s) for the author(s) of this article can be found under:  
<https://doi.org/10.1002/anie.201708524>.

with Au, Pt, and Ag electrodes show the opposite trend to what we observe. We reason that the different bonding or electrostatic environment inherent to measurements with monolayer compared with single-molecule measurement gives rise to the different results.

Additionally, we find that Pt-Si<sub>n</sub>-Pt junctions show the lowest conductance compared with Ag-Si<sub>n</sub>-Ag and Au-Si<sub>n</sub>-Au junctions. This result stands in contrast to previous theoretical studies<sup>[12]</sup> on benzene-dithiol and experimental studies<sup>[5c]</sup> on alkane-dithiol, both of which show that the conductance of single molecule junctions formed with Pt electrodes is higher than that of the molecular junctions formed with other metal contacts such as Au or Ag. Our results from measurements with three different metals indicate that conductance trends across different metals are not simply related to work function trends (Ag: 4.64 eV; Au: 5.47 eV; Pt: 5.84 eV).<sup>[13]</sup>

Si<sub>2</sub>-Si<sub>4</sub> and Si<sub>6</sub> were synthesized through an iterative route, as described previously.<sup>[14]</sup> We extended this approach to synthesizing the longer hepta-, octa-, and nona-silane (Si<sub>7</sub>-Si<sub>9</sub>) oligomers presented here (details provided in the Supporting Information). We carried out conductance measurements by repeatedly breaking and forming Ag, Au, and Pt point contacts in the presence of a solution of target molecules using a STM-BJ technique.<sup>[7]</sup> The STM is operated under ambient condition at room temperature for Ag and Au measurements. For measurements with Pt, we additionally polish and sonicate the Pt slug in acetone and flush the setup chamber with argon for 10 minutes prior to the measurement. We use mechanically polished Ag and Pt slug and Au-coated mica surface as the substrate, and the corresponding metal wire as the tip.

We initiate each measurement by bringing the tip into contact with the substrate to create a metal point contact with a conductance higher than 5G<sub>0</sub> (G<sub>0</sub> = 2e<sup>2</sup>h<sup>-1</sup> = 77.5 μS), then we retract the tip while measuring the current and the voltage of the junction. A molecule in the vicinity can bridge the gap between the tip and substrate once the metal point-contact breaks (Figure 1a), displaying a plateau in the conductance versus displacement trace (Figure S1 in the Supporting Information). We collected 4000–20000 conductance traces for each molecular junction and compile them into normalized log-binned conductance histograms. Histograms for the amine-linked Si<sub>4</sub> and thiol-linked Si<sub>6</sub> with Au and Ag electrodes are shown in Figure 1b,c; others are shown in Figure S2. We generate conductance histograms for molecular junctions formed with Au and Pt electrodes without any data selection, and apply an automated algorithm to exclude the traces displaying long oxygen contamination plateaus<sup>[15]</sup> between 1G<sub>0</sub> and 0.1G<sub>0</sub> before creating the histograms for junctions formed with Ag electrodes (see Figure S3 for complete histograms). As an additional control, we have measured the conductance of thiol-terminated alkanes in an argon environment and do not find any change in the molecular conductance peak position (Figure S4). For the Pt measurements, we note that we do not observe a conductance peak at 1G<sub>0</sub> in agreement with previous reports.<sup>[5b,16]</sup> This has been explained by calculations showing that transport in Pt atomic contacts, unlike the single fully open channel 6s for Au, has contributions from its d-bands.<sup>[5b,16]</sup>

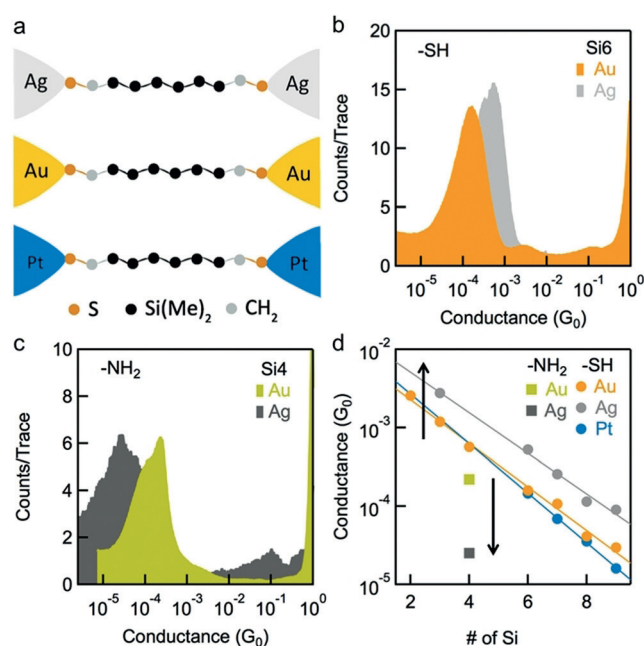


**Figure 1.** a) Schematic representation of thiol-linked metal-Si<sub>n</sub>-metal junctions. 1D logarithmically binned conductance histograms for junctions of: b) thiol-terminated Si<sub>6</sub> and c) amine-terminated Si<sub>4</sub> with Au and Ag electrodes. d) Conductance peak values plotted against the number of silicon atoms in the backbone on a semi-log scale. Lines show linear fits to the data following  $G = G_c e^{-\beta n}$  and corresponding decay constants  $\beta$  are  $0.64 \pm 0.02 \text{ n}^{-1}$  for Au,  $0.60 \pm 0.03 \text{ n}^{-1}$  for Ag, and  $0.73 \pm 0.02 \text{ n}^{-1}$  for Pt. Arrows indicate higher conductance for Ag electrodes with thiol-linked junctions, and lower conductance for Ag electrodes with amine-linked junctions.

We fit Gaussian functions to the conductance peaks in the histograms to determine the most probable conductance value for each silane bound to Ag/Au/Pt metal contacts. We plot the conductance value as a function of the number of silicon atoms in the backbone in Figure 1d. We first find that the conductance of thiol-linked junction decreases exponentially as the molecular length increases. Comparing the conductance for each silane bound to Au and Ag electrical contacts, we find that thiol-linked junctions show higher conductance when formed with Ag electrodes, while amine-linked ones show a lower conductance when formed with Ag electrodes (as indicated by arrows in Figure 1d). Interestingly, we observe the same trends in amine-terminated<sup>[4b]</sup> and thiol-terminated alkanes. (Figure S5) This result suggests that the anchoring groups, when attached to different metal contacts, can significantly alter the charge transport characteristics. We also observe that molecular junctions formed with Pt electrodes have the lowest conductance.

We create 2D conductance-displacement histograms to further compare the junction elongation length measured with different metal contacts. These histograms, shown in Figure 2a,b and Figures S5 and S6, are created by overlaying all measured conductance traces after aligning them along the displacement axis at a conductance of 0.5 G<sub>0</sub> (Au and Ag) or 0.01 G<sub>0</sub> (Pt). We compare the molecular-junction plateau shapes and lengths between measurements with the three metal contacts. We find that Au-Si<sub>n</sub>-Au and Ag-Si<sub>n</sub>-Ag

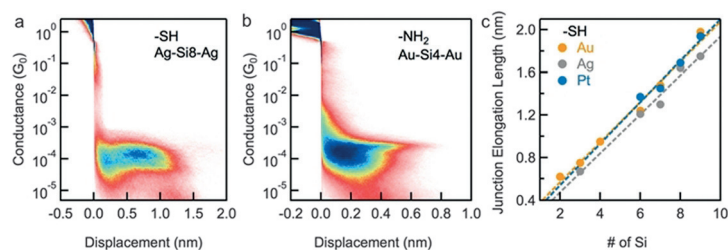


**Figure 2.** 2D conductance histograms for a) Si<sub>8</sub>-SH measured with Ag and b) Si<sub>4</sub>-NH<sub>2</sub> measured with Au. c) Junction elongation length plotted against the number of silicon atoms in the backbone for measurements with thiol-linked junctions with Ag, Au, and Pt electrodes.

junctions show similar conductance vs. displacement distribution, while for Pt-Si<sub>n</sub>-Pt junctions, the start of the conductance plateau is not well defined owing to the lack of a sharp conductance drop following the metal contact rupture (Figure S6). We determine the junction elongation length from the 2D histogram (details provided in the Supporting Information Part III) and plot them as a function of the backbone length for measurements with Au, Ag, and Pt electrodes in Figure 2c. A linear increase in the measured junction elongation length with increasing backbone length is observed in measurements of the thiol-terminated silanes with all three metal contacts, indicating that we are indeed forming junctions that are terminally bound through a Au-S, Ag-S, or Pt-S bond.

To gain insight into the charge-transfer characteristics of these junctions, we turn to quantum transport calculations of model junctions with different anchoring groups attached to Au and Ag electrodes. In our *ab initio* study we employ density functional theory as implemented in the FHI-aims package<sup>[17]</sup> with a PBE exchange-correlation functional.<sup>[18]</sup> Scalar relativistic corrections are included at the atomic ZORA (zeroth order regular approximation) level.<sup>[19]</sup> To validate ZORA, additional calculations with TURBOMOLE (scalar relativistic, ECP-level) have been performed (see Supporting Information). Spectral effects of the spin-orbit interaction are treated by performing a single-shot post-processing diagonalization of the Kohn-Sham Hamiltonian including the spin-orbit interaction term.<sup>[20]</sup> Each pyramidal cluster of Au (Ag) contains 37 atoms and is cut from a face-centered crystal grown in the (111) direction with closest interatomic distance of 2.88 Å (2.89 Å). Transport calculations employ a standard non-equilibrium Green's function method as implemented in the quantum transport package AITRANSS.<sup>[21]</sup>

We show in Figure 3 the transmission of junctions of Si<sub>4</sub> and Si<sub>7</sub> bound to Ag and Au electrodes through amine and thiol linkers. In all cases, the HOMO level dominates the charge transport, and its width and alignment with the metal Fermi energy determines the conductance. In the case of amine-linked junctions, the essential difference between Au and Ag contacts is a rigid displacement of the transmission curve by about 0.4 eV (Figure 3a). This shift in the transmission curves is consistent with experimental values for the work function mismatch, which is approximately 0.6 eV for the corresponding facets.<sup>[13,22]</sup>

The situation is considerably more intricate with thiol linkers. We first observe that the overall conductance is enhanced in comparison to the amine-case, because the transport-orbitals are in better alignment with the Fermi energy. The enhancement is stronger for Ag electrodes (factor ca. 5) when compared to Au (factor ca. 4), in qualitative agreement with experiment (Figure 1d). This difference results from two factors: i) After replacing amines with thiols, the relative shift of the HOMO peaks for Au- and Ag-based junctions is only about 0.1 eV, substantially smaller than the work function differ-

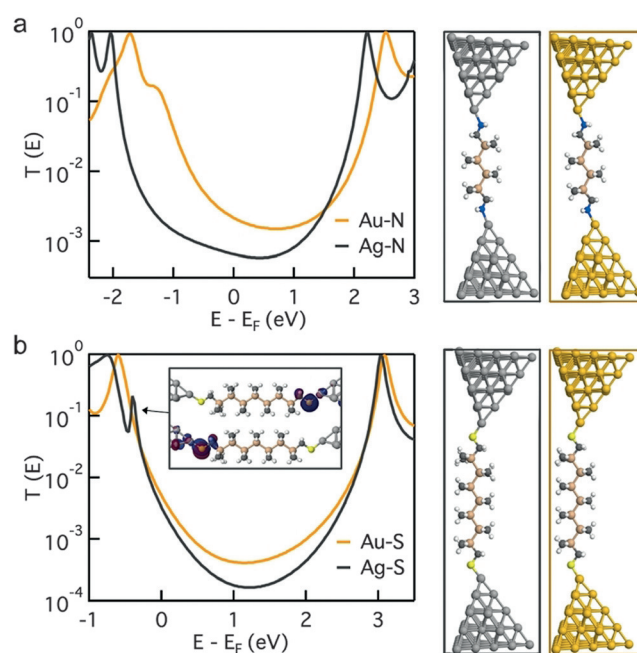


**Figure 3.** Calculated transmission curves and molecular structures for Au and Ag junctions formed with a) Si<sub>4</sub> with amine linker groups and b) Si<sub>7</sub> with thiol linkers. Inset: Gateway state orbitals. HOMO and LUMO orbitals are shown in Figures S7–S10.

ence; ii) In Ag-based junctions an extra resonance appears at 400 meV below the Fermi energy, attributed to a Ag-S orbital gateway state. In Au-linked junctions however, the gateway state is close to the broadened HOMO orbital and therefore is not visible as a separate resonance.<sup>[23]</sup> Despite the gateway orbital being located mostly near the thiol-group, it carries a significant contribution of the current as the corresponding (narrow) resonance energy is close enough to the Fermi energy and outside of the broadened HOMO peak.

In conclusion, we find that silicon molecular wires terminated with thiol linkage groups show higher conductance with Ag electrodes than with Au electrodes, in contrast, the ones terminated with amine linkage groups show the opposite trend. These results highlight the impact of the chemical linkers on determining the charge-transport characteristics of molecular junctions when attached to different metal contacts. We show that as a consequence of the different chemical properties of the anchoring group, the

conductance trends at the Fermi level for different metals may not follow simple rules based on the metal work-function. Our supporting DFT calculations suggest an understanding that invokes i) the alignment between the molecular HOMO and the Fermi level of the metal, ii) the gateway states as important factors influencing the conductance trends in both thiol-linked and amine-linked junctions. Additionally, we demonstrate that Pt can be used as the metal to form molecular junctions with thiol-terminated silanes and that Pt-Si<sub>n</sub>-Pt shows even lower conductance than Au-Si<sub>n</sub>-Au junctions. Our results open up the possibilities of using Ag and Pt as electrical contacts in molecular electronics and deepen our understanding of the role that the metal–molecule interaction plays in controlling molecular conductance.

### Acknowledgements

Discussions with A. Donarini are gratefully acknowledged. We thank NSF for support of experimental studies under grant no. CHE-1404922 (H.L.). M.C.-G. was supported by the Deutsche Forschungsgemeinschaft via GRK 1570. T.A.S. was supported by the NSF Graduate Research Fellowship under grant no. 11–44155. R.K. and V.P. acknowledge the support of the PRIMUS/Sci/09 program of the Charles University. M.S.I. was supported by a Marie Skłodowska Curie Global Fellowship (M.S.I., MOLCLICK: 657247) within the Horizon 2020 Programme.

### Conflict of interest

The authors declare no conflict of interest.

**Keywords:** metal–molecule interactions · silanes · silver · platinum · single-molecule electronics

**How to cite:** *Angew. Chem. Int. Ed.* **2017**, *56*, 14145–14148  
*Angew. Chem.* **2017**, *129*, 14333–14336

- [1] a) E. M. van Schroyen Lantman, T. Deckert-Gaudig, A. J. G. Mank, V. Deckert, B. M. Weckhuysen, *Nat. Nanotechnol.* **2012**, *7*, 583; b) J. Zhang, M. B. Vukmirovic, Y. Xu, M. Mavrikakis, R. R. Adzic, *Angew. Chem. Int. Ed.* **2005**, *44*, 2132; *Angew. Chem.* **2005**, *117*, 2170.
- [2] a) D.-Y. Wu, X.-M. Liu, S. Duan, X. Xu, B. Ren, S.-H. Lin, Z.-Q. Tian, *J. Phys. Chem. C* **2008**, *112*, 4195; b) N. E. Christensen, *J. Phys. F* **1978**, *8*, L51.
- [3] a) P. Pyykko, J. P. Desclaux, *Acc. Chem. Res.* **1979**, *12*, 276; b) O. Adak, R. Korytár, A. Y. Joe, F. Evers, L. Venkataraman, *Nano Lett.* **2015**, *15*, 3716.
- [4] a) S. Kaneko, T. Nakazumi, M. Kiguchi, *J. Phys. Chem. Lett.* **2010**, *1*, 3520; b) T. Kim, H. Vázquez, M. S. Hybertsen, L. Venkataraman, *Nano Lett.* **2013**, *13*, 3358; c) Z.-L. Peng, Z.-B. Chen, X.-Y. Zhou, Y.-Y. Sun, J.-H. Liang, Z.-J. Niu, X.-S. Zhou, B.-W. Mao, *J. Phys. Chem. C* **2012**, *116*, 21699; d) Y.-H. Wang, D.-F. Li, Z.-W. Hong, J.-H. Liang, D. Han, J.-F. Zheng, Z.-J. Niu, B.-W. Mao, X.-S. Zhou, *Electrochem. Commun.* **2014**, *45*, 83.
- [5] a) M. Kiguchi, O. Tal, S. Wohlthat, F. Pauly, M. Krieger, D. Djukic, J. C. Cuevas, J. M. van Ruitenbeek, *Phys. Rev. Lett.* **2008**, *101*, 046801; b) T. Yelin, R. Korytar, N. Sukenik, R. Vardimon, B. Kumar, C. Nuckolls, F. Evers, O. Tal, *Nat. Mater.* **2016**, *15*, 444; c) C.-H. Ko, M.-J. Huang, M.-D. Fu, C.-h. Chen, *J. Am. Chem. Soc.* **2010**, *132*, 756.
- [6] a) Y.-H. Wang, X.-Y. Zhou, Y.-Y. Sun, D. Han, J.-F. Zheng, Z.-J. Niu, X.-S. Zhou, *Electrochim. Acta* **2014**, *123*, 205; b) Y.-H. Wang, Z.-W. Hong, Y.-Y. Sun, D.-F. Li, D. Han, J.-F. Zheng, Z.-J. Niu, X.-S. Zhou, *J. Phys. Chem. C* **2014**, *118*, 18756.
- [7] B. Xu, N. J. Tao, *Science* **2003**, *301*, 1221.
- [8] C. D. Bain, E. B. Troughton, Y. T. Tao, J. Evall, G. M. Whitesides, R. G. Nuzzo, *J. Am. Chem. Soc.* **1989**, *111*, 321.
- [9] V. B. Engelkes, J. M. Beebe, C. D. Frisbie, *J. Am. Chem. Soc.* **2004**, *126*, 14287.
- [10] Z. Xie, I. Bâldea, C. E. Smith, Y. Wu, C. D. Frisbie, *ACS Nano* **2015**, *9*, 8022.
- [11] B. Kim, S. H. Choi, X. Y. Zhu, C. D. Frisbie, *J. Am. Chem. Soc.* **2011**, *133*, 19864.
- [12] a) J. W. Lawson, C. W. Bauschlicher, *Phys. Rev. B* **2006**, *74*, 125401; b) W. T. Geng, J. Nara, T. Ohno, *Thin Solid Films* **2004**, *464–465*, 379.
- [13] J. Hölzl, F. Schulte in *Solid Surface Physics*, Springer, Heidelberg, **1979**, p. 1.
- [14] H. Li, T. A. Su, V. Zhang, M. L. Steigerwald, C. Nuckolls, L. Venkataraman, *J. Am. Chem. Soc.* **2015**, *137*, 5028.
- [15] Y. Qi, D. Guan, Y. Jiang, Y. Zheng, C. Liu, *Phys. Rev. Lett.* **2006**, *97*, 256101.
- [16] L. Cui, W. Jeong, S. Hur, M. Matt, J. C. Klöckner, F. Pauly, P. Nielaba, J. C. Cuevas, E. Meyhofer, P. Reddy, *Science* **2017**, *355*, 1192–1195.
- [17] V. Blum, R. Gehrke, F. Hanke, P. Havu, V. Havu, X. Ren, K. Reuter, M. Scheffler, *Comput. Phys. Commun.* **2009**, *180*, 2175.
- [18] J. P. Perdew, K. Burke, M. Ernzerhof, *Phys. Rev. Lett.* **1996**, *77*, 3865.
- [19] E. van Lenthe, E. J. Baerends, J. G. Snijders, *J. Chem. Phys.* **1994**, *101*, 9783.
- [20] W. P. Huhn, V. Blum, *Phys. Rev. Materials*, **2017**, *1*(3), 033803.
- [21] a) A. Arnold, F. Weigend, F. Evers, *J. Chem. Phys.* **2007**, *126*, 174101; b) A. Bagrets, *J. Chem. Theory Comput.* **2013**, *9*, 2801.
- [22] H. L. Skriver, N. M. Rosengaard, *Phys. Rev. B* **1992**, *46*, 7157.
- [23] C. Li, I. Pobelov, T. Wandlowski, A. Bagrets, A. Arnold, F. Evers, *J. Am. Chem. Soc.* **2008**, *130*, 318.

Manuscript received: August 18, 2017

Accepted manuscript online: September 22, 2017

Version of record online: October 6, 2017